Original Article

Evaluation of Axillary Lymph Node Status in Breast Cancer with MRI

Goro Yoshimura, Takeo Sakurai, Syoji Oura, Takaomi Suzuma, Takeshi Tamaki, Teiji Umemura, Yozo Kokawa, and Qifeng Yang

Background: We performed a retrospective study to establish the optimal radiological criteria for axillary lymph node metastases from breast cancer by measuring all dissected nodes, and to determine whether magnetic resonance imaging (MRI) could reliably reveal axillary involvement.

Methods: Pathological findings and MRI scans of 202 patients with invasive breast cancer were reviewed. The long- and short-axis dimensions of all level I and II lymph nodes were measured microscopically, and then the long-to-short axis (L/S) ratio of each node was calculated. These parameters were compared with pathological nodal status to define radiological criteria for axillary involvement. MRI was carried out using T1-weighted spin-eho sequences in the coronal and sagittal planes. On MRI, every detected lymph node was measured and the shape of the nodal cortex was also examined. Then the diagnostic ability of MRI was assessed using these morphologic criteria.

Results: On histopathological examinations of 4043 dissected lymph nodes, a long-axis dimension of 10 mm or larger combined with a long-to-short axis ratio of less than 1.6 was the most accurate criteria for predicting lymph node metastases. On MRI, eccentric cortical hypertrophy was seen in only metastatic axillae. When these morphologic features were used as criteria for malignancy, MRI had a sensitivity of 79%, a specificity of 93%, and an accuracy of 88%. In 16 of 17 false-negative axillae, MRI showed normally sized lymph nodes (<10 mm).

Conclusion: Our study indicates that MRI is a useful diagnostic method for the evaluation of axillary nodal status, but is limited in the detection of small metastatic lymph nodes.

Breast Cancer 6:249-258, 1999.

Key words: Breast cancer, Axillary lymph node metastases, Radiological criteria, MRI

With the growing implementation of breast cancer screening programs, a shift in the spectrum of breast cancer towards smaller tumors has been made[1]. The trend in loco-regional treatment of breast cancer has become more and more conservative in the last few decades. For several years the role of routine axillary dissection has been questioned due to the relatively low incidence of axillary lymph node metastasis in patients with small tumors, potential morbidity, cost, and lack of significant therapeutic value[2-5]. In Japan, however, axillary lymph node dissection remains a mainstay of surgical treatment.

Attempts at axillary staging by means of direct imaging of the axilla with mammography, ultrasonography (US), and computed tomography (CT) have proved more useful than clinical examination[6-10]. Radiological criteria for metastatic nodes have been as follows: dense nodes of increased attenuation and spiculated contour on mammography[6], a short-axis dimension greater than 10 mm on CT[10], a long-axis dimension greater than 5 mm on US[7,8], and a round-shaped node with a long-axis dimension greater than 5 mm on US[9]. In most of these studies, an approach which predicts lymph node status by assessing the size and shape of the lymph node is generally accepted. There has not been an agreement on the criteria for identifying metastatic nodes.

Magnetic resonance imaging (MRI) has been reported by several authors to significantly improve the accuracy of detecting metastatic lymph

Department of Surgery, Kihoku Hospital, Wakayama Medical College.
Reprint requests to Goro Yoshimura, Department of Surgery, Kihoku Hospital, Wakayama Medical College, 219, Katsuragi, Ito-gun, Wakayama 649-7113, Japan.

Abbreviations:
MRI, Magnetic resonance imaging; US, Ultrasonography; CT, Computed tomography; L/S ratio, Long-to-short axis ratio

Received December 25, 1998; accepted June 9, 1999

nodes from head and neck cancer, esophageal cancer, and pelvic neoplasms[11-13]. To date, there have been very few reports on the ability of MRI to evaluate lymph node status of the low axilla in breast cancer.

The purpose of this study was to measure level I and II lymph nodes in 202 axillary dissections and to assess the relationship between nodal size and shape and presence of metastasis. We also wanted to determine whether MRI could reliably reveal axillary node metastases by size and shape. In addition, other MRI morphologic criteria including differences of signal intensity and changes of lymph node internal structure were analyzed.

Material and Methods

At Wakayama Medical College, Kihoku Hospital between April 1995 and December 1997, 261 breast cancer patients were examined preoperatively with MRI scanning. Patients who did not undergo lymph node dissection, patients with noninvasive carcinoma and patients with distant metastases were excluded, leaving 202 for analysis.

Table 1. Patient Characteristics

Age	30-86 years (mean 55)
Menopausal status	
Premenopausal	103
Postmenopausal	99
Tumor size (cm)	
≦2.0	76
2.1-5.0	110
≧5.1	16
Histologic type[a]	
Papillotubular	60
Solid-tubular	49
Scirrhous	67
Others	26
Axillary dissection	
I II	37
I II III	165
Clinical nodal status	
Negative	141
Positive	61
Histologic nodal status	
Negative	122
Positive	
1-3	44
4-9	19
>10	17

[a]Histologic type is according to the classification of the Japanese Breast Cancer Society.

Patient and tumor characteristics are presented in Table 1. All patients underwent fine-needle aspiration cytology of the palpable breast mass before MRI scanning. Age ranged from 30 to 86 years, with a mean of 55 years. Of the 202 patients, 178 underwent modified radical mastectomy (nipple preserving mastectomy[14] in 166), and the remaining 24 were treated with a breast conserving procedure, quadrantectomy plus axillary dissection. Complete axillary dissection of all three levels was performed in 165 patients. The remaining 37 had level I and II dissection.

The lymph nodes were dissected from the fresh axillary specimens, and each lymph node was embedded and sectioned along its largest axial plane. A hematoxylin-eosin (HE) stain was used to verify the presence of nodal metastases. All the level I and II lymph nodes were measured along the long- and short-axis dimension on microscopic slides, and then the long-to-short axis (L/S) ratio of each node was calculated.

Magnetic resonance examinations were performed on a 1.5-tesla superconducting magnet system (SIGNA; GE Medical Systems, Milwaukee, WI). For axillary examinations, the patient was supine and the arms were fixed in a hyperabducted position with the hands under the head. A 3-inch standard circular surface coil (GE Medical Systems) was used. A T1-weighted spin-eho sequence was performed in the coronal and sagittal oblique planes of the level I and II regions (Fig 1). The sequence parameters were 300 ms/12 ms (repetition time/echo time); 128×256 matrix size; 16 cm field of view; two excitations; 3 mm slice thickness without a gap. Fourteen images were obtained in approximately 3 min from each plane. Every MRI-detected lymph node was measured along the long- and short-axis dimension of the maximal cut surface on MRI, and then the L/S ratio was calculated. The long-axis dimension and the L/S ratio of the largest lymph node in each axilla were analyzed to determine the relationship between pathological and preoperative MRI findings. In addition, other morphologic features such as differences in signal density and the shape of the peripheral cortex were evaluated on MRI.

Differences between the sizes of benign and malignant nodes were analyzed using Student's *t* test. We analyzed the correlation between the measured pathological and MRI size by simple regression analysis. All statistical analysis was

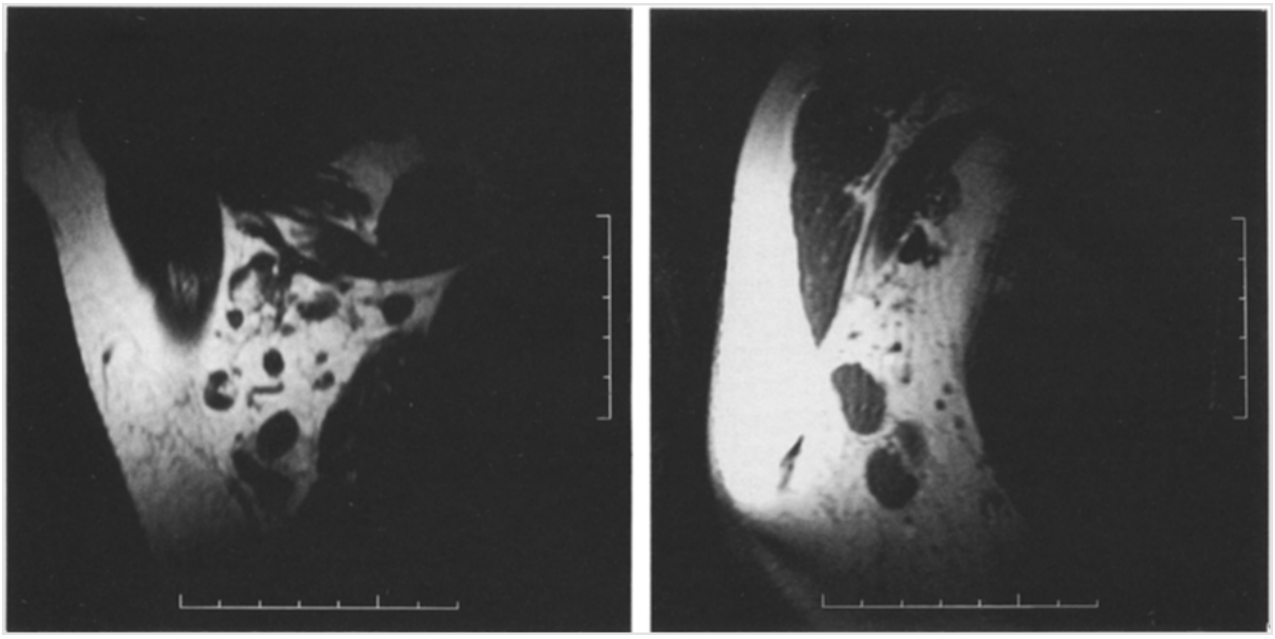

Fig 1. Axillary lymph node metastases in a 47-year-old woman. Left, Coronal T1-weighted spin-echo image. Right, Slightly angulated sagittal T1-weighted image. Images show multiple lymph nodes ranging from 3 mm to 20 mm in size at level I and II.

calculated using StatView-J 4.5 software (Abacus Concepts, Inc, Berkeley, CA). Sensitivity was computed as the number of true-positive cases/(number of true-positive+false-negative cases)×100. Specificity was computed as the number of true-negative cases/(number of true-negative+false-positive cases)×100. The positive predictive value was computed as the number of true-positive cases/(number of true-positive+false-positive cases)×100. The negative predictive value was computed as the number of true-negative cases/(number of true-negative+false-negative cases)×100.

Results

Pathological Findings

Of the 202 axillae, 80 (40%) had lymph node metastases. There was no case with metastatic involvement at level Ⅲ or the interpectoral region without lymph node metastases at level Ⅰ and Ⅱ. Of the 80 positive axillae, 44 axillae had 1 to 3 positive nodes, 19 axillae had 4 to 9 positive nodes, and the remaining 17 axillae had 10 or more positive nodes.

A total of 4043 lymph nodes were located at level Ⅰ or Ⅱ with an average of 20 per case (range 3 to 45), and were examined. These nodes could be divided after histological evaluation into 3528 negative nodes and 515 positive nodes. The mean long-axis dimension in the 515 positive nodes was significantly larger than that of the 3528 negative nodes (7.6±5.0 mm and 4.1±2.4 mm, respectively; $p<0.0001$). Of the negative nodes, 3435 (97%) were less than 10 mm in maximum dimensions. The distribution in size of the positive nodes showed greater variation, and 378 of the

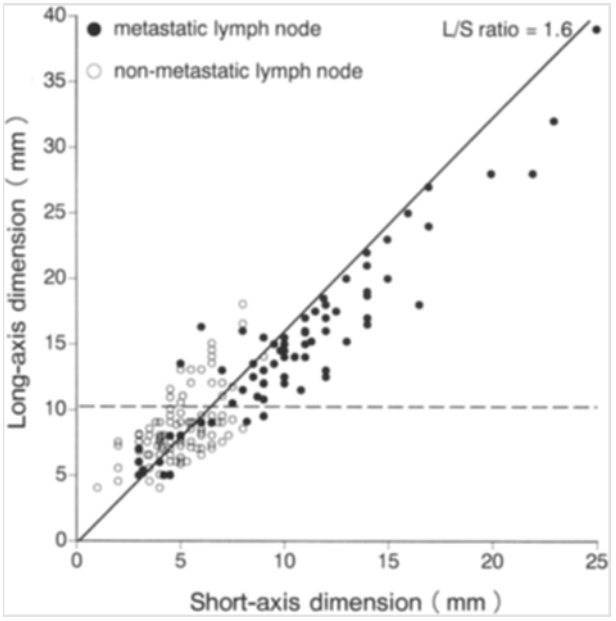

Fig 2. The long-axis dimension versus the short-axis dimension of the largest lymph in each axilla on pathological examination.

positive nodes (73%) measured less than 10 mm. The percentage of positive nodes less than 10 mm (positive nodes less than 10 mm/all positive nodes) was 41% (28/69) in the 44 axillae with 1 to 3 metastatic nodes, 71% (82/116) in the 19 axillae with 4 to 9 metastatic nodes, and 81% (268/330) in the 17 axillae with more than 10 metastatic nodes. The mean L/S ratio of the positive nodes was significantly smaller than that of the negative nodes (1.484 ± 0.368 and 1.694 ± 0.621, respectively; $p < 0.0001$). There was also a large range of overlap in the L/S ratio between positive and negative nodes. No statistical criterion for metastases could be drawn from these analyses.

Therefore, the largest node in each axilla was studied. Figure 2 represents the distribution of the long and short-axis dimension for the largest negative and positive nodes. From this diagram, it is apparent that the majority of positive axillae had a long-axis dimension of 10 mm or larger and a L/S ratio of 1.6 or less. Table 2 shows the sensitivity, specificity, positive predictive value, negative predictive value, and accuracy of the size criterion (a long-axis dimension $\geqq 10$ mm), the shape criterion (a L/S ratio < 1.6), and the size combined with the shape (a long-axis dimension $\geqq 10$ mm and a L/S ratio < 1.6). In the 202 axillae, the combined criteria yielded an accuracy of 89% compared with 80% for the size criterion alone, and 67% for the shape criterion alone. There were 18

Table 2. Sensitivity, Specificity, Predictive Values, and Accuracy for Several Criteria on Pathological Examinations

	Sensitivity	Specificity	Predictability		Accuracy
			Positive	Negative	
Size[a] $\geqq 10$ mm	84%	78%	71%	88%	80%
L/S ratio < 1.6	86%	54%	55%	86%	67%
Size[a] $\geqq 10$ mm combined with L/S tatio < 1.6	78%	96%	93%	87%	89%

[a]Long-axis dimension.

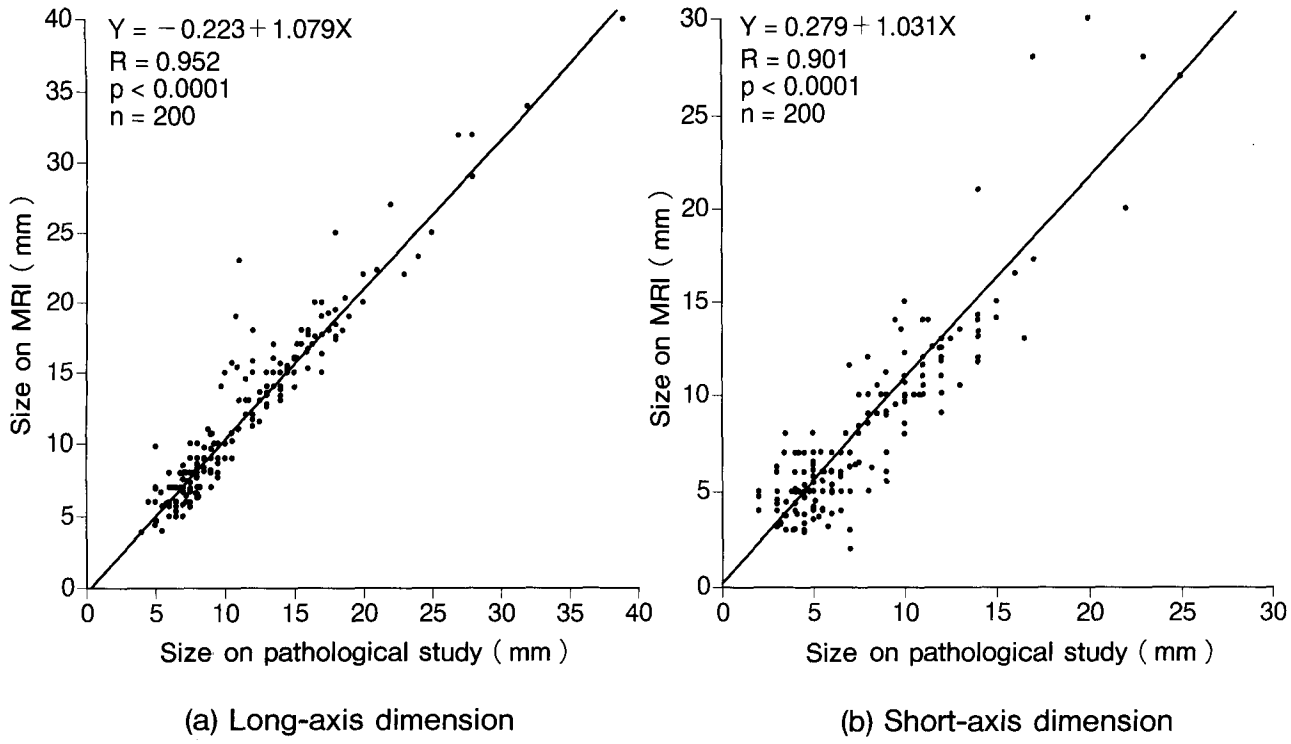

Fig 3. Correlation between size of the largest lymph node in each axilla on MRI and pathological examination for the long-axis (a) and the short-axis dimension (b).

false-negative axillae using the combined criteria. Ten axillae had 1 to 3 nodes with only micrometastases (the size of tumor involvement was less than 2 mm within the lymph node); the remaining 8 axillae had macrometastatic disease (larger than 2 mm).

Correlation between Pathological and MRI-Measured Size

MRI detected lymph nodes in 200 of the 202 axillae (99%). Two axillae in which MRI showed no lymph node were histologically negative. A total of 1400 lymph nodes were visualized on MRI, and the number per axilla ranged from 0 to 25 with a mean of 7.0 ± 4.8.

The long- and short-axis dimensions of the largest node in each axilla on MRI were compared with measurements from microscopic slides. The mean long- and short-axis dimension on the microscopic slides was 11.2 ± 5.3 mm and 7.3 ± 4.0 mm, respectively. The mean long- and short-axis dimension on MRI was 11.9 ± 6.0 mm and 7.8 ± 4.6 mm, respectively. Figure 3 shows the relationship between the size of the largest node in each axilla on pathological examination and MRI. Both the long- and short-axis dimensions showed significant correlation between the pathological size and the MRI-measured size (long-axis dimension, $r=0.952$, $p<0.0001$; short-axis dimension, $r=0.901$, $p<0.0001$).

A lymph node of 10 mm or larger with a L/S ratio of less than 1.6 on MRI (Fig 4) was found in 59 of the 80 pathologically positive axillae (74%).

Other Morphologic Features on MRI

Of the 200 axillae with lymph nodes visualized by T1-weighted MRI, 103 showed all axillary nodes with a homogenous low signal intensity regardless of metastatic disease. In some patients spin-echo T2-weighted images were also performed (Fig 5). The signal intensity of each lymph node on T2-weighted images was homogenous, and there were no significant differences between metastatic and non-metastatic nodes. We were therefore unable to differentiate malignant from benign nodes with signal intensity.

Ninety-seven axillae showed one to several lymph nodes with a fatty hilus of high signal intensity and a cortex of low intensity. Of the 97 axillae, 27 had lymph nodes with eccentric cortical hypertrophy on MRI, and all were pathologically malignant (Figs 6 and 7). Thirty-eight axillae had lymph nodes with a C-shaped cortex (usually 1 to 2 mm thick), and 26 of the 38 axillae (68%) were pathologically benign (Fig 8). In the remaining 32 axillae, we could not evaluate the shape of the cortex because the lymph nodes were small (<10 mm).

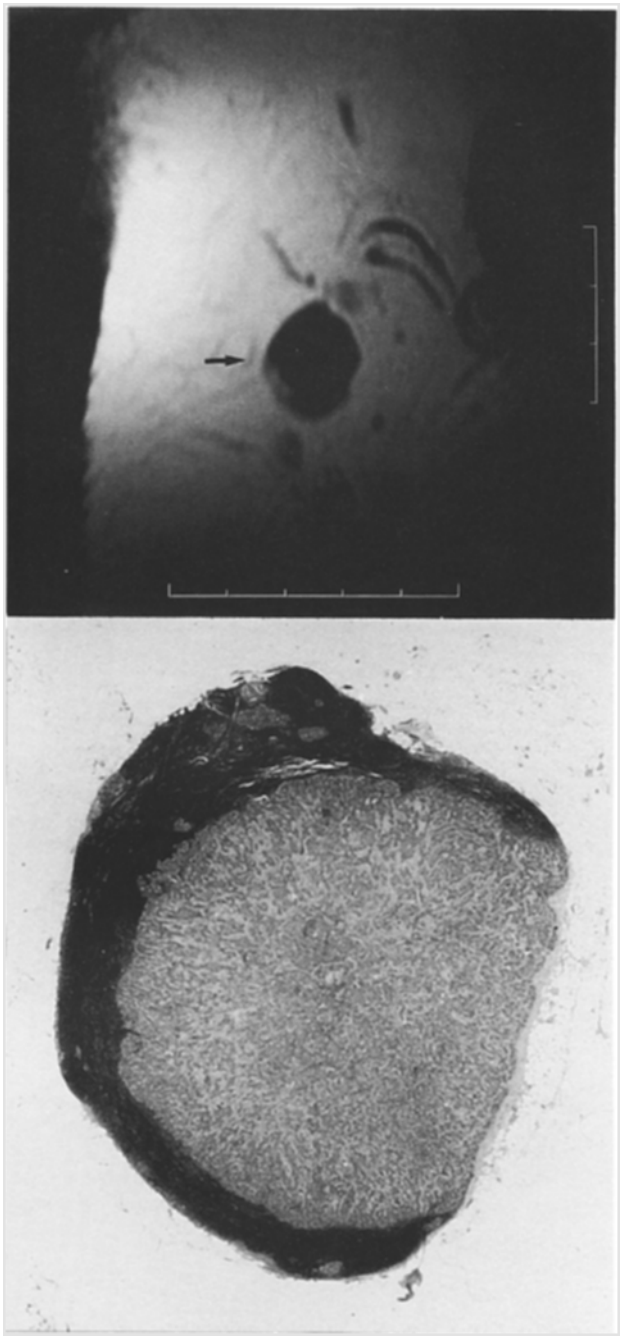

Fig 4. Top, T1-weighted coronal image obtained from a 45-year-old woman shows a lymph node 20 mm in long-axis dimension with a L/S ratio of 1.25 (arrow). Bottom, Histopathological slice shows that the structure is totally involved with neoplastic disease (HE, original magnification ×6).

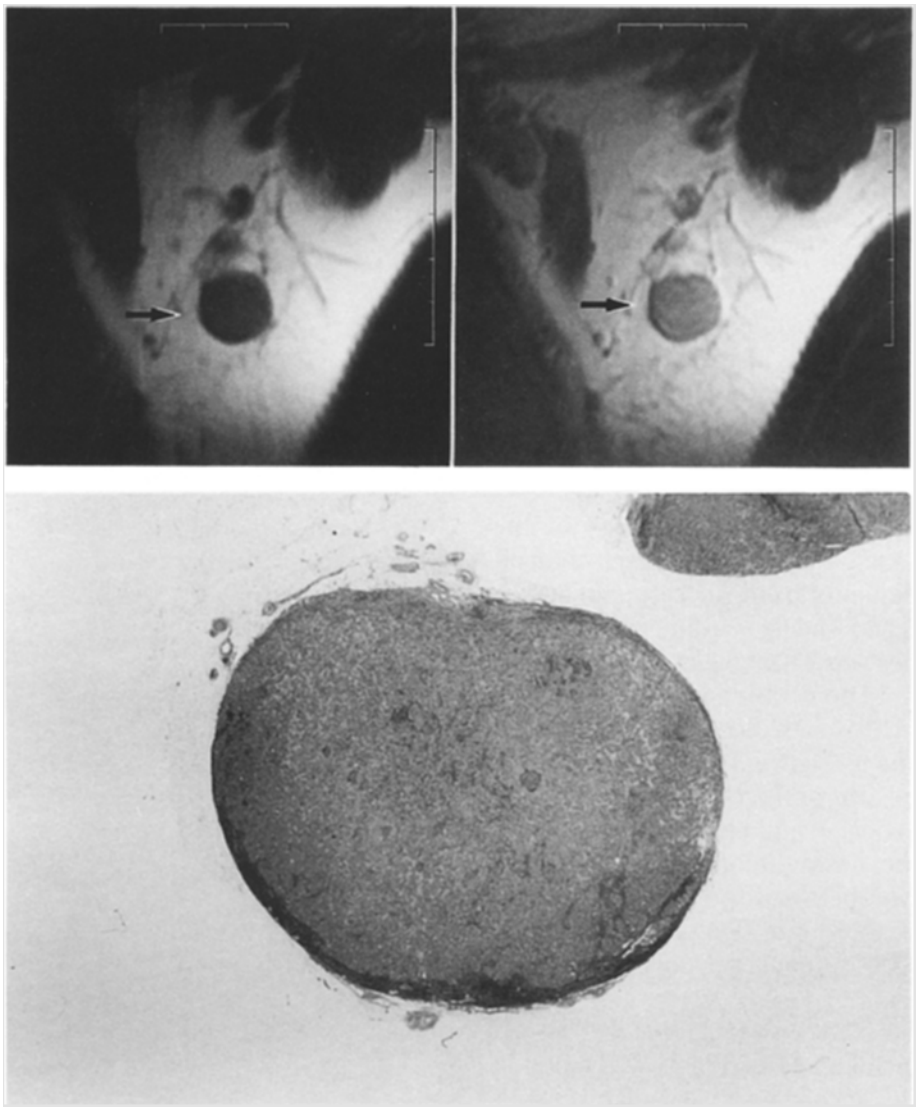

Fig 5. Images obtained from a 57-year-old woman show a metastatic lymph node (arrow). Top left, T1-weighted coronal image. Top right, T2-weighted coronal image. Homogenous nodal enlargement is seen on both images. Bottom, Histopathological slice shows total involvement of the lymph node (HE, original magnification ×6).

Criteria for Lymph Node Involvement on MRI

On MRI, lymph nodes measuring 10 mm or larger with a L/S ratio of less than 1.6 were considered to harbor metastasis. A further criterion for malignancy was eccentric cortical hypertrophy. MRI accurately predicted lymph node involvement in 63 of the 80 positive axillae. Of 17 false-negative axillae on MRI, 10 had micrometastatic lymph nodes and the remaining 7 had macrometastatic diseases. In all but one of these cases, MRI showed normally sized (< 10 mm) lymph nodes.

The results of MRI findings are presented in Tables 3 and 4. The sensitivity, specificity, positive predictability, negative predictability, and accuracy of MRI was 79%, 93%, 89%, 87%, and 88% respectively. All of these values were higher than those obtained with clinical examination.

Discussion

To date there is little information regarding the relationship between nodal size and the presence of metastasis in breast cancer. In our series, 73% of the metastatic lymph nodes were less than 10 mm. Most of these small positive nodes occurred with multiple other nodes larger than 10

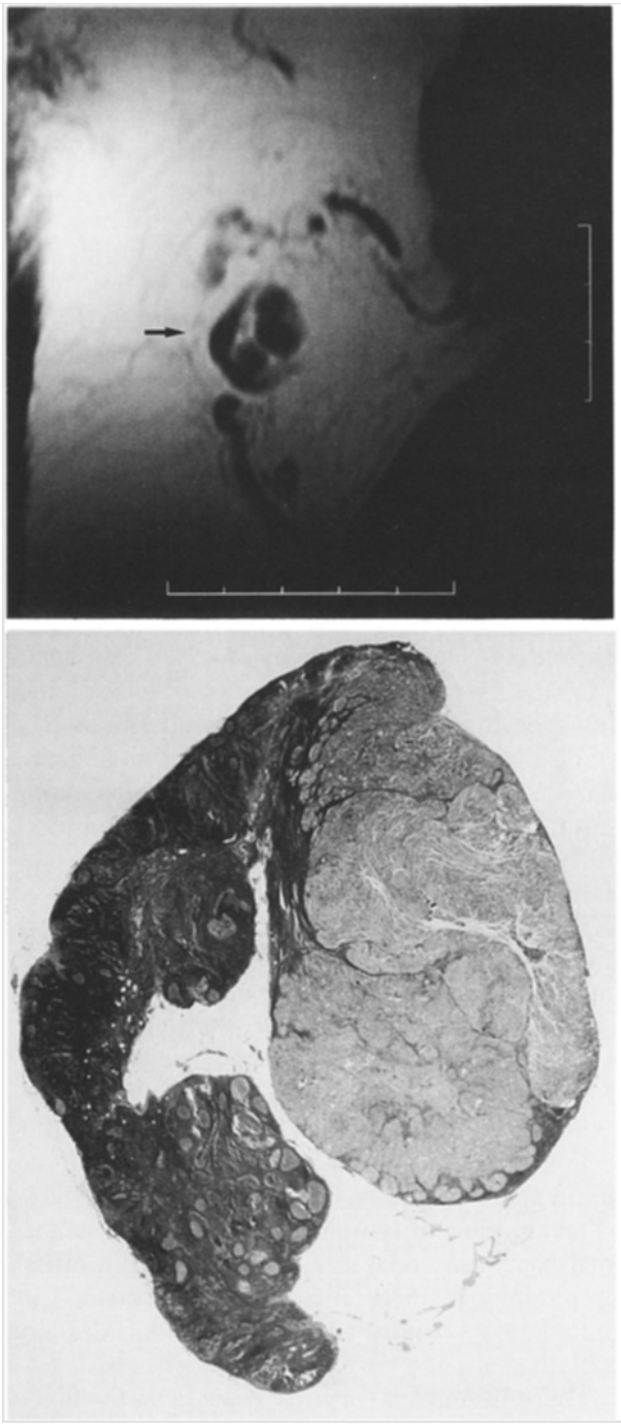

Fig 6. Top, T1-weighted coronal image obtained from a 45-year-old woman shows a lymph node with segmental enlargement of the cortex (arrow). Bottom, Histopathologically, this area is composed of metastatic tissue (HE, original magnification ×6).

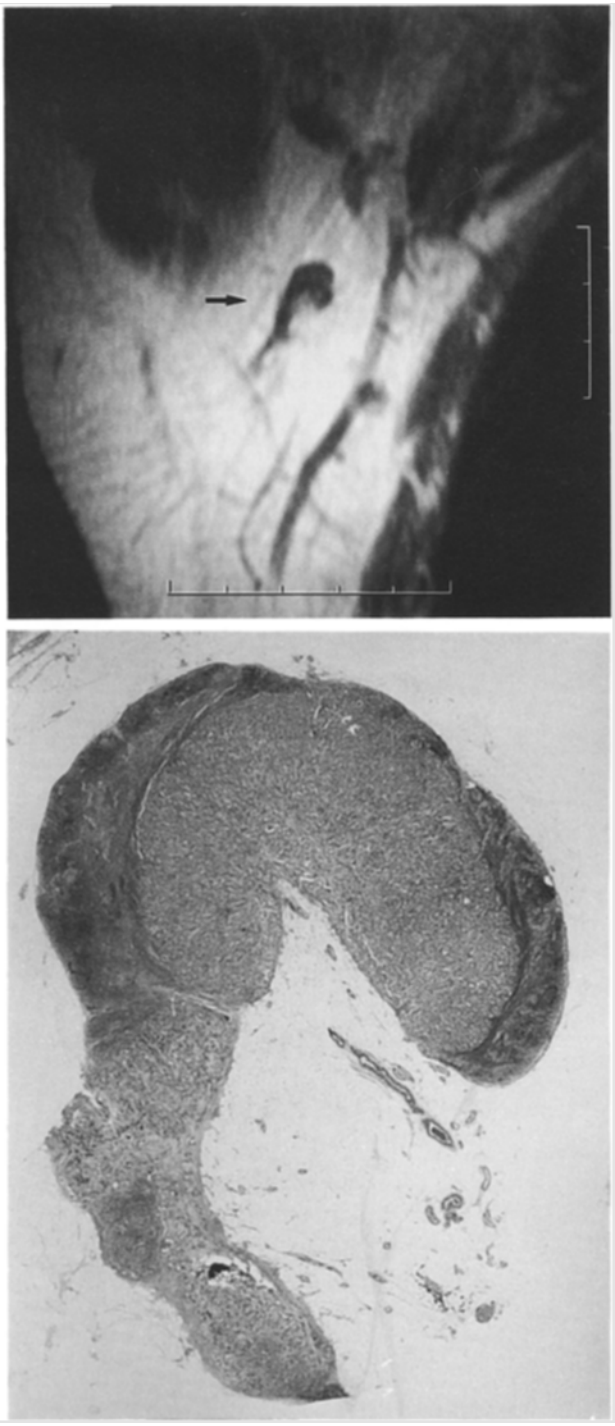

Fig 7. Top, T1-weighted coronal image obtained from a 51-year-old woman shows a flat-shaped lymph node with eccentric widening of the cortex (arrow). Bottom, Histopathological slice shows peripheral replacement of nodal tissue by tumor (HE, original magnification ×8).

mm. Therefore, we studied axillary lymph node status using the largest node per axilla as a marker of involvement. Our pathological study indicated that combining size and shape (a long-axis dimension $\geqq$10 mm and a L/S ratio $<$1.6) more accurately predicted tumor-positive axillae than size or shape alone. US studies of cervical lymph node metastases from head and neck cancer have

also demonstrated that combining size and shape increased accuracy[15,16].

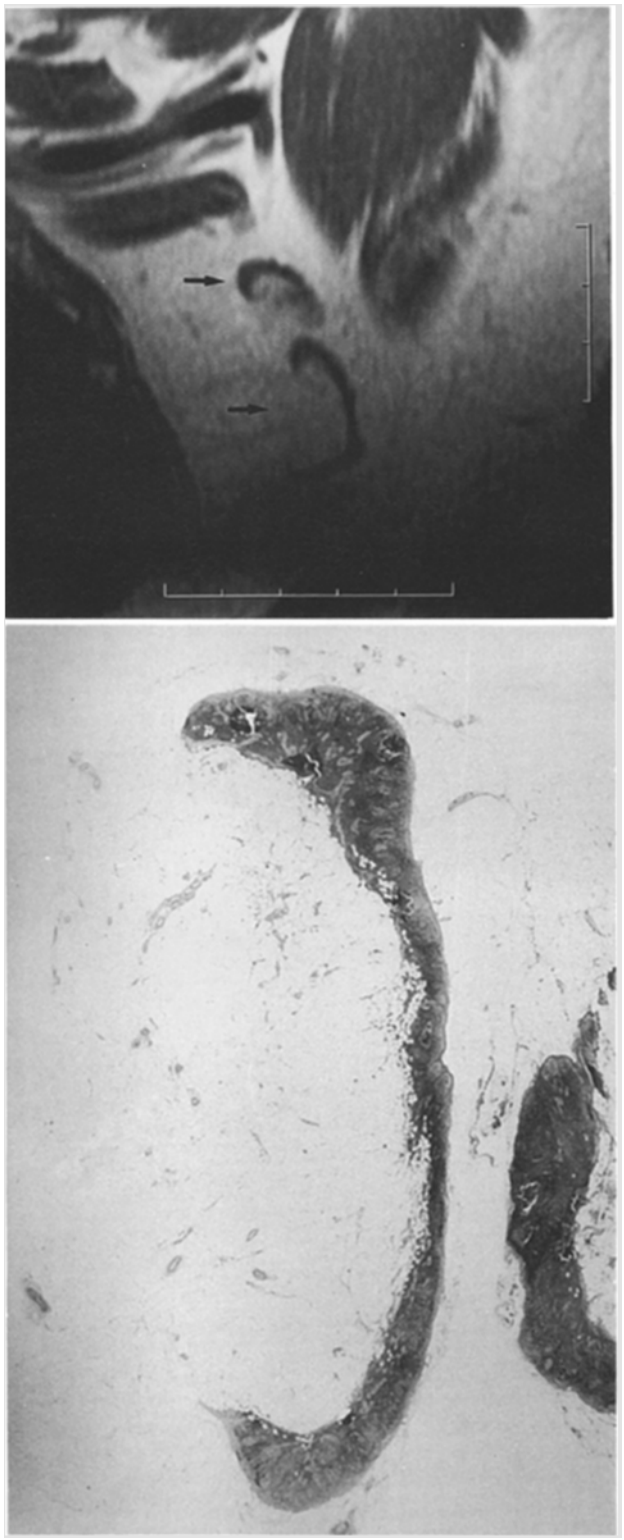

Fig 8. Top, T1-weighted coronal image obtained from a 64-year-old woman shows C-shaped lymph nodes (arrow). Bottom, Histopathological slice shows the peripheral cortex and fatty replacement of the central hilus without metastatic tissue (HE, original magnification ×8).

Clinical examination for lymph node involvement is notoriously unreliable, with an overall error rate of 39% and a false-negative rate of up to 45%[17]. Direct imaging techniques of the axilla, such as US and CT, have been applied to improve the detection of disease in the axilla.

US has frequently been used in the past for axillary lymph node imaging. US studies, in which the criterion for detection of involved nodes was 5 mm or larger in maximal dimension, showed a sensitivity of 69% to 73%, a specificity of 70% to 97%, and an accuracy of 71% to 88%[7-9]. Recent studies have shown that high-resolution US enables differentiation between benign and malignant nodes using ultrasonomorphologic features. An *in vitro* US study by Feu *et al*[21] has suggested that tumor involvement may result in a round shape, absence of the hilus, and disruption of the cortex. Yang *et al*[22] reported that high-resolution US had a sensitivity of 84%, a specificity of 97%, and an accuracy of 92% using these signs. However, it is difficult with US to distinguish a lymph node from the surrounding tissues, especially in the axillary region which contains abundant fat[23]. In recent studies using high-resolution US, lymph nodes could be detected in only 50-60% of the examined axillae[24,25].

Studies analyzing the efficacy of CT have been fewer than US. March *et al*[10] reported that CT had a sensitivity of 50%, a specificity of 75% and an accuracy of 55% using the size criterion of 10 mm of the short-axis dimension. In Japan, Ogawa *et al*[26] regarded lymph nodes of larger than 5 mm in a short-axis dimension as malignant on 5-mm section CT images, and reported a sensitivity of 90%, a specificity of 86% and an accuracy of 88%. CT evaluation of lymph node involvement has been based on nodal size only, and not on other morphologic features. It is well known that CT is limited in its ability to evaluate nodal size on axial images alone[18-20].

There have been very few reports on the ability of MRI to detect axillary lymph node involvement. Fossel *et al*[27] have suggested that proton T1

Table 3. Correlation between Evaluation of MRI and Histologic Nodal Status

	Histology negative	Histology positive
MRI negative	114	17
MRI positive	8	63

Table 4. MRI Compared with Clinical Examination as a Predictor of Axillary Lymph Node Involvement

	Sensitivity	Specificity	Predictability		Accuracy
			Positive	Negative	
MRI examination	79%	93%	89%	87%	88%
Clinical examination	61%	90%	80%	78%	79%

values may help distinguish benign from malignant lymph nodes in an *in vitro* study. In a number of studies by Yoshimoto *et al*[28,29], MRI evaluation of lymph nodes at the parasternal, level III and interpectoral regions has been found to be useful for detection of metastatic nodes. To our knowledge, there has been no previous report to assess the diagnostic value of lymph node metastases at level I and II with MRI. Our study showed that one or more lymph nodes were visualized on MRI in 200 of the 202 axillae (99%). T1-weighted MRI can display axillary lymph nodes more clearly than US or CT images, because they provide excellent tissue contrast between the low intensity lymph nodes and the high intensity fat. Hergan *et al*[30] reported that MRI would appear to be the best method for showing normal anatomy and its relation to pathology. Because MR images can be thinly sliced in the sagittal and coronal planes, nodal size can be determined accurately. Moreover, if the lymph node is 10 mm or larger, MRI can evaluate a change in the shape of the cortex. Using the criteria of enlarged size with round shape and eccentric cortical hypertrophy for malignancy, the sensitivity, specificity and accuracy of MRI was 79%, 93%, and 88% respectively. Because of differences in study populations, it is difficult to compare our results using MRI with studies using other imaging modalities. MRI is thought to be more accurate than CT for measuring nodal size. US is cheaper and more easily available than MRI, but US is dependent on the examiner's skill and documentation may be difficult. We consider MRI to be as useful as US for the assessment of axillary nodal metastases.

Despite the accurate assessment of enlarged lymph nodes, MRI is not helpful in detecting metastatic nodes of normal size. In 16 of the 17 false-negative axillae in our MRI examinations, lymph nodes were less than 10 mm. Because metastases may occur in normally sized and shaped nodes, the overall accuracy for criteria based on these morphologic features cannot be 100% with any imaging techniques. Of interest are the recent studies that have documented the capacity of iron oxide contrast agent to improve the sensitivity of MRI in the detection of lymph node metastases for head and neck cancer. Anzai *et al*[31] reported that non-metastatic nodes reduced their signal intensity significantly following dextran-covered superparamagnetic iron oxide administration. The use of this contrast media or imaging with a special pulse sequence may overcome the current difficulties, but this needs further clinical investigation.

Sentinel node biopsy has been employed to accurately assess the axillary nodal status, and the majority of recent studies reported that the accuracy of this procedure was more than 95%[32-35]. Veronesi *et al*[33] state that axillary dissection may be unnecessary when the sentinel node is disease-free. Generally, sentinel node biopsy has been applied to patients with clinically negative axillae. However, clinical examination is unreliable. In our opinion, sentinel node biopsy should be performed in cases of negative findings on reliable imaging techniques, including MRI. Furthermore, we believe that MRI is the best imaging technique to follow patients without axillary dissection when the sentinel node is negative.

Conclusion

MRI is a useful diagnostic method for identifying axillary lymph node involvement, because excellent anatomic detail permits accurate evaluation of nodal size and shape. However, MRI has a significant limitation in the detection of metastatic nodes with normal size. New methods for addressing this important clinical issue are sorely needed.

References

1) Tabar L, Fagerberg G, Day N, *et al*: Breast cancer treatment and natural history; New insights from results of screening. *Lancet* 339:412-414, 1992.

2) Chadha M, Chabon AB, Friedmann P, *et al*: Predictors of axillary lymph node metastases in patients with T1 breast cancer. *Cancer* 73:350-353, 1994.
3) Fein DA, Fowble BL, Hanlon AL, *et al*: Identification of women with T1-T2 breast cancer at low risk of positive axillary nodes. *J Surg Oncol* 65:34-39, 1997.
4) Barth A, Craig PH, Silverstein MJ: Predictors of axillary lymph node metastases in patients with T1 breast carcinoma. *Cancer* 79:1918-1922, 1997.
5) Cady B: The need to reexamine axillary lymph node dissection in invasive breast cancer. *Cancer* 73:505-508, 1994.
6) Dershaw DD, Panicek DM, Osborne MP: Significance of lymph nodes visualized by the mammographic axillary view. *Breast Dis* 4:271-280, 1991.
7) Bruneton JN, Caramella E, Hery M, *et al*: Axillary lymph node metastases in breast cancer; Preoperative detection with US. *Radiology* 158:325-326, 1986.
8) Vaidya JS, Vyas JJ, Thakur MH, *et al*: Role of ultrasonography to detect axillary node involvement in operable breast cancer. *Eur J Surg Oncol* 22:140-143, 1996.
9) Pamilo M, Soiva M, Lavast EM: Real-time ultrasound, axillary mammography, and clinical examination in the detection of axillary lymph node metastases in breast cancer patients. *J Ultrasound Med* 8:115-120, 1989.
10) March DE, Wechsler RJ, Kurtz AB, *et al*: CT-pathologic correlation of axillary lymph nodes in breast carcinoma. *J Comput Assist Tomogr* 15:440-444, 1991.
11) Som PM: Detection of metastasis in cervical lymph nodes; CT and MR criteria and differential diagnosis. *Am J Roentgenol* 158:961-969, 1992.
12) Lehr L, Rupp N, Siewart JR: Assessment of resectability of oesphageal cancer by computed tomography and magnetic resonance imaging. *Surgery* 103:344-350, 1988.
13) Jager GJ, Barentsz JO, Oosterhof GO, *et al*: Pelvic adenopathy in prostatic and urinary bladder carcinoma; MR imaging with a three-dimensional T1-weighted magnetization-prepared rapid gradient-echo sequence. *AJR* 167:1503-1507, 1996.
14) Oura S: A clinical study of nipple preserved radical mastectomy; It is safetiness in the preservation of nipple-areola complex on breast cancer operation. *J Wakayama Med Soc* 45:525-536, 1994 (in Japanese with English abstract).
15) Som PM: Lymph nodes of the neck. *Radiology* 165: 593-600, 1987.
16) Close LG, Merkel M, Vuitch MF, *et al*: Computed tomographic evaluation of regional lymph node involvement in cancer of the oral cavity and oropharynx. *Head Neck* 11:309-317, 1989.
17) Sacre RA: Clinical evaluation of axillary lymph nodes compared to surgical and pathological findings. *Eur J Surg Oncol* 12:169-175, 1986.
18) Lein HH, Hindskold L, Stenwig AE, *et al*: Shape of retroperitoneal lymph nodes at computed tomography does not correlate to metastatic disease in early stage non-seminomatous testicular tumors. *Acta Radiologica* 28:271-273, 1987.
19) Takeshi A, Matsumoto T, Kuramitu T, *et al*: Is it possible differentiate malignant mediastinal nodes from benign nodes by size? *Chest* 110:1004-1008, 1996.
20) Vassallo P, Edel G, Roos N, *et al*: In-vitro high-resolution ultrasonography of benign and malignant lymph nodes; A sonographic-pathologic correlation. *Invest Radiol* 28:698-705, 1993.
21) Feu J, Tresserra F, Fabregas R, *et al*: Metastatic breast carcinoma in axillary lymph nodes; In vitro US detection. *Radiology* 205:831-835, 1997.
22) Yang WT, Ahuja A, Tang A, *et al*: High resolution sonographic detection of axillary lymph node metastases in breast cancer. *J Ultrasound Med* 16:241-246, 1996.
23) Marchal G, Oyen R, Verschakelen J, *et al*: Sonographic appearance of normal lymph nodes. *J Ultrasound Med* 4:417-419, 1985.
24) Verbanck J, Vandewiele I, De Winter H, *et al*: Value of axillary ultrasonography and sonographically guided puncture of axillary nodes; A prospective study in 144 consecutive patients. *J Clin Ultrasound* 25:53-56, 1997.
25) Bonnema J, van Geel AN, van Ooijen B, *et al*: Ultrasound-guided aspiration biopsy for detection of nonpalpable axillary node metastases in breast cancer patients; New diagnostic method. *World J Surg* 21: 270-274, 1997.
26) Ogawa Y, Nishioka A, Hamada N, *et al*: Recent progress of imaging diagnosis for breast cancer; Role of CT and/or Helical CT for breast cancer. *Jpn J Breast Cancer* 11:243-253, 1996 (in Japanese with English abstract).
27) Fossel ET, Brodsky G, Delayre JL, *et al*: Nuclear magnetic resonance for the differentiation of benign and malignant breast tissues and axillary lymph nodes. *Ann Surg* 198:541-545, 1983.
28) Yoshimoto M, Iwase T, Watanabe S, *et al*: Magnetic resonance imaging and metastatic pattern of the internal mammary lymph nodes of breast cancer. *Jpn J Breast Cancer* 6:221-227, 1991 (in Japanese with English abstract).
29) Yoshimoto M, Iwase T, Kasumi F: Diagnostic accuracy of axillary lymph node metastases in breast cancer by palpation and diagnostic imaging. *Jpn J Breast Cancer* 10:460-467, 1995 (in Japanese with English abstract).
30) Hergan K, Morrigl B, Kathrein A, *et al*: MR and CT anatomy of the axilla. *Acta Radiologica* 38:198-205, 1997.
31) Anzai Y, Blackwell KE, Hirshowitz SL: Initial clinical experience with dextran-coated superparamagnetic iron oxide for detection of lymph node metastases in patients with head and neck cancer. *Radiology* 192: 709-715, 1994.
32) Albertini JJ, Lyman GH, Cox C, *et al*: Lymphatic mapping and sentinel node biopsy in the patient with breast cancer. *JAMA* 276:1818-1822, 1996.
33) Veronesi U, Paganelli G, Galimberti V, *et al*: Sentinel node biopsy to avoid axillary dissection in breast cancer with clinically negative lymph-nodes. *Lancet* 349: 1864-1867, 1997.
34) Giuliano AE, Jones RC, Brennan M, *et al*: Sentinel lymphadenectomy in breast cancer. *J Clin Oncol* 15: 2345-2350, 1997.
35) Krag D, Weaver D, Ashikaga T, *et al*: The sentinel node in breast cancer. *N Engl J Med* 339:941-946, 1998.